

Available online at www.sciencedirect.com

ScienceDirect

journal homepage: www.e-jds.com

Original Article

Targeting MetaLnc9/miR-143/FSCN1 axis inhibits oxidative stress and myofibroblast transdifferentiation in oral submucous fibrosis

Ming-Yi Lu ^{a,b}, Pei-Ling Hsieh ^c, Shih-Chi Chao ^{d,e},
Chih-Yuan Fang ^{f,g}, Yoichi Ohiro ^h, Yi-Wen Liao ^{d,e},
Cheng-Chia Yu ^{a,b,d**}, Min-Te Chang ^{i*}

^a School of Dentistry, Chung Shan Medical University, Taichung, Taiwan

^b Department of Dentistry, Chung Shan Medical University Hospital, Taichung, Taiwan

^c Department of Anatomy, School of Medicine, China Medical University, Taichung, Taiwan

^d Institute of Oral Sciences, Chung Shan Medical University, Taichung, Taiwan

^e Department of Medical Research, Chung Shan Medical University Hospital, Taichung, Taiwan

^f Division of Oral and Maxillofacial Surgery, Department of Dentistry, Wan Fang Hospital, Taipei, Taiwan

^g School of Dentistry, College of Oral Medicine, Taipei Medical University, Taipei, Taiwan

^h Oral and Maxillofacial Surgery, Division of Oral Pathobiological Science, Faculty of Dental Medicine and Graduate School of Dental Medicine, Hokkaido University, Sapporo, Japan

ⁱ Department of Oral and Maxillofacial Surgery, Chi-Mei Medical Center, Tainan, Taiwan

Received 1 April 2024; Final revision received 10 April 2024

Available online 23 April 2024

KEYWORDS

Oral submucous
fibrosis;
MetaLnc9;
miR-143;
FSCN1

Abstract *Background/purpose:* Persistent activation of myofibroblasts is attributed to various dysregulated biological events conferring multiple types of fibrosis diseases, including oral submucous fibrosis (OSF). Although the significance of non-coding RNAs (ncRNAs) in the occurrence of fibrosis has been appreciated, the detailed mechanisms still have not been fully elucidated. The aim of this study was to identify key dysregulated ncRNAs and elucidate their pro-fibrotic mechanisms in promoting myofibroblast activation and the pathological development of OSF.

Materials and methods: Expression of non-coding RNAs and mRNAs in OSF cohort was determined using RNA sequencing and qRT-PCR. The molecular axis of pro-fibrotic ncRNAs were

* Corresponding author. Department of Oral and Maxillofacial Surgery, Chi-Mei Medical Center, No. 901, Zhonghua Rd. Yongkang Dist., Tainan 71004, Taiwan.

** Corresponding author. Institute of Oral Sciences, Chung Shan Medical University, No. 110, Sec. 1, Jianguo N. Rd., Taichung 40201, Taiwan.

E-mail addresses: ccyu@csmu.edu.tw (C.-C. Yu), penette2@gmail.com (M.-T. Chang).

<https://doi.org/10.1016/j.jds.2024.04.008>

1991-7902/© 2024 Association for Dental Sciences of the Republic of China. Publishing services by Elsevier B.V. This is an open access article under the CC BY-NC-ND license (<http://creativecommons.org/licenses/by-nc-nd/4.0/>).

exploited via luciferase reporter activity assay and RNA expression rescue experiments. Functional assays, including collagen gel contraction, wound healing ability, cell migration, and reactive oxygen species (ROS) production, were conducted to assess the changes in the myofibroblastic phenotypes of primary human buccal mucosal fibroblasts.

Results: Herein, we found that long non-coding RNA MetaLnc9 was upregulated in OSF specimens and positively associated with several fibrosis markers. Silencing of MetaLnc9 diminished the features of activated myofibroblasts and the production of ROS. We not only showed that MetaLnc9 functioned as a competitive endogenous RNA of microRNA (miR)-143, but also demonstrated that the pro-fibrosis effect of MetaLnc9 on myofibroblast activities was mediated by suppression of miR-143. Moreover, our data showed that fascin actin-bundling protein 1 (FSCN1) was a direct target of miR-143 and positively related to MetaLnc9.

Conclusion: Upregulation of MetaLnc9 may enhance the activation of myofibroblasts by sponging miR-143 and titrating its inhibitory property on FSCN1.

© 2024 Association for Dental Sciences of the Republic of China. Publishing services by Elsevier B.V. This is an open access article under the CC BY-NC-ND license (<http://creativecommons.org/licenses/by-nc-nd/4.0/>).

Introduction

As a progressive and irreversible fibrosis disease, oral sub-mucous fibrosis (OSF) has long been recognized as a pre-malignant disorder of oral cancer. Although the pathogenesis of OSF is multifactorial and remains largely unexplored, myofibroblast transdifferentiation from human buccal mucosal fibroblasts (BMFs) following chronic exposure to the constituent of areca nuts seems to be a crucial etiological event.¹ Considering the excessive deposition of extracellular matrix (ECM) proteins is attributed to the resident fibroblast-derived myofibroblasts, a better understanding of the molecular mechanism underlying myofibroblast transdifferentiation of BMFs is essential for the treatment of this fibrosis condition.

Accumulating evidence suggests that non-coding RNAs (ncRNAs) are central regulators of myofibroblast differentiation, and their aberrant expression confers various types of fibrosis diseases.^{2,3} One of the possible modes of lncRNA (>200 bp ncRNA) functionality is to serve as competitive endogenous RNAs (ceRNAs) or 'sponges' of microRNAs (miRNA; ~19–24 bp ncRNA) that can bind to complementary sites in the 3' prime untranslated region (3'UTR) of target mRNAs and cause degradation.⁴ By decreasing the availability of miRNAs to target genes, these ceRNAs can regulate gene expression post-transcriptionally. In fact, several studies have demonstrated that this ceRNA network is implicated in orchestrating the development of OSF.^{5,6} Given that individual miRNAs may modulate an abundance of genes, more work is warranted to dissect the ceRNA regulatory network in order to acquire a comprehensive understanding.

MetaLnc9, also known as LINC00963, was first found in prostate cancer cells and associated with the capacity of cancer metastasis.^{7,8} Previous studies reported that MetaLnc9 can function as a ceRNA to regulate tumor progression of various types of cancer.^{9–11} Most importantly, it has been found that aberrant overexpression of MetaLnc9 is related to cancer stemness, metastasis, and drug resistance of oral cancer.¹¹ However, its effect on the development of precancerous OSF has not been investigated. Of note, it has

been revealed that MetaLnc9 inhibits the TGF- β 1-elicited myofibroblast transdifferentiation of corneal fibroblasts as well as lowers the secretion of collagen I and III by down-regulating miR-143-3p.¹² As such, it is intriguing to inspect whether MetaLnc9 is pro-fibrosis or anti-fibrosis during myofibroblast transdifferentiation of BMFs and associated molecular mechanisms.

Materials and methods

Subsection

Collection of normal and fibrotic buccal mucosa specimens were carried out respectively from healthy and OSF individuals undergoing resection at the Department of Dentistry, Chung Shan Medical University Hospital. The procedures were as according to the one approved by the Institutional Review Board in Chung Shan Medical University Hospital, Taichung, Taiwan. Prior to the procedures, all informed written consent from each individual were obtained. The extraction of normal BMFs and fibrotic fBMFs (fBMFs) were done from the normal and fibrotic buccal mucosa specimens of the same patients, respectively. Cells were routinely maintained in Dulbecco's Modified Eagle's Medium (DMEM) containing 10% fetal bovine serum (FBS) and 1% penicillin–streptomycin with 5% CO₂ at 37 °C, and passages 3–8 were used. The details of primary cell isolation, identification, and culture were as previously described.⁵ All reagents were purchased from ThermoFisher Scientific (Waltham, MA, USA).

Silencing MetaLnc9 through lentiviral-mediated knockdown system

The pLV-RNAi vector was obtained from Biosettia Inc. (San Diego, CA, USA), and cloning of the double-stranded shRNA sequence followed the manufacturer's protocol. The oligonucleotide sequence targeting human MetaLnc9 was synthesized and cloned into pLV-RNAi to create a lentiviral expression vector. The target sequences for MetaLnc9 are

as follows: Sh- MetaLnc9-1 5'-AAAAGGCGCAGTAACAATA-TAATTTGGATCCAAATTATATTGTTACTGCGCC -3'; MetaLnc9-2 5'-AAAAGCTCACTGAACCTTTCTGAATTGGATCCAATTCA-GAAAGTTCAGTGAGC -3. Lentivirus production involved co-transfection of the plasmid DNA mixture with the lenti-vector and helper plasmids (VSVG and Gag-Pol) into 293T cells (ATCC, Manassas, VA, USA) using Lipofectamine 2000 (LF2000, Invitrogen) according to the manufacturer's protocol.¹³ Unless explicitly stated otherwise, the transfection reagent used in following experiments was Lipofectamine 2000.

Quantitative reverse transcription polymerase chain reaction

Clinical specimens were prepared by immediately placing surgically excised tissues into liquid nitrogen and storing them at -80°C . Total RNA was extracted from tissues and cells using Trizol reagent following the manufacturer's protocol (Invitrogen). mRNA was reverse-transcribed using the Superscript III first-strand synthesis system (Invitrogen). Quantitative reverse transcription polymerase chain reaction (qRT-PCR) were conducted on resulting cDNAs using the ABI StepOne™ Real-Time PCR Systems (Applied Biosystems, Foster City, CA, USA). Primer sequences used were: α -SMA (forward: 5'-AGCACATGGAAAAGATCTGGCACC-3', reverse: 5'-TTTCTCCCAGTTGGCCTTG-3'), COL1A1 (forward: 5'-GGGTGACCGTGGTGAGA-3', reverse: 5'-CCAGGAGAGCCA-GAGGTCC-3'), and GAPDH (forward: 5'-CTCATGACCA-CAGTCCATGC-3', reverse: 5'-TTCAGCTCTGGGATGACCTT-3').¹³

MicroRNA mimic and inhibition

To modulate the expression of endogenous miR-143, cells were transfected with miR-143 mimic or miR-143 inhibitor. The miR-scramble served as a negative control. Quantification of miR-143 levels was conducted using qRT-PCR with TaqMan miRNA assays employing specific primer sets (Applied Biosystems).¹³ All oligonucleotides were purchased from ThermoFisher Scientific.

Collagen contraction assay

Cells were mixed with 0.5 ml of 2 mg/ml collagen solution (MilliporeSigma, St. Louis, MO, USA) and placed into a single well of a 24-well plate. The plate was then incubated at 37°C for 2 h to allow the gels to polymerize. Polymerized gels were carefully detached from the wells and transferred to fresh medium in a 24-well plate for further 48 h of incubation. Contraction of the gels was documented and quantified by measuring their areas using ImageJ software (National Institutes of Health, Bethesda, MD, USA).¹⁴

Wound healing assay

When cell confluence reached 80% in a 12-well culture plate, a denuded area was generated by carefully scratching the cell monolayer using a sterile 200 μL pipette tip across the center of the well. Cell migration towards the

wound area was assessed using a microscope at 0 and 48 h.¹⁴

Transwell migration assay

Cells were seeded into the upper chamber of transwell inserts (Corning Inc., Corning, NY, USA) containing serum-free medium. Medium supplemented with 10% fetal bovine serum was added to the lower chamber to act as a chemoattractant. Following an additional 48 h of incubation, cells that had migrated to the underside of the membrane were stained with 0.1% crystal violet and counted in 5 randomly selected fields under a microscope.¹⁴

Reactive oxygen species production analysis

Intracellular ROS production was evaluated using flow cytometry by measuring the fluorescence of 2',7'-dichlorofluorescein (DCF), the oxidation product of 2',7'-dichlorodihydrofluorescein diacetate (DCFH-DA). Cells were incubated with 10 μM DCFH-DA (Invitrogen) for 60 min at 37°C , followed by two washes with PBS. The fluorescence of DCF in 10,000 cells was analyzed using flow cytometry (Becton Dickinson, Franklin Lakes, NJ, USA) at 488/525 nm (excitation/emission).¹⁵

Western blotting

Whole-cell lysates were prepared using NP-40 lysis buffer (MilliporeSigma). Twenty-five μg of total protein from the lysates underwent separation by 10% sodium dodecyl sulfate polyacrylamide gel electrophoresis and were subsequently transferred onto a polyvinylidene difluoride membrane (MilliporeSigma). Following blocking with 5% bovine serum albumin, the membranes were incubated with specific primary antibodies and corresponding secondary antibodies. GAPDH as internal standards for quantifying protein levels. Immunoreactive bands were visualized using ECL-plus chemiluminescence substrate (MilliporeSigma) and captured with a LAS-1000plus Luminescent Image Analyzer (GE Healthcare Biosciences, Chicago, IL, USA). Quantification of the bands was performed using ImageJ software (National Institutes of Health). Antibodies were sourced from ThermoFisher Scientific.

MicroRNA-targeting gene prediction and dual-luciferase reporter assay

The wild-type MetaLnc9-3'UTR was inserted into the β -galactosidase (β -gal) control plasmid following the manufacturer's instructions (Promega, Madison, WI, USA). To create the mutant reporter, the original sequence UCAUCUC in the wild-type reporter was replaced with AGUAGAG. The β -gal activity of the vector alone plasmid (VA), the wild-type (Wt) reporter, and the mutant (Mut) reporter were normalized using the luciferase activity of a co-transfected plasmid expressing luciferase to account for background reporter activity. The reporter plasmid was co-transfected with either miR-143 mimic or miR-Scramble into cells. Firefly luciferase activity, normalized to

transfection efficiency, served as a measure of reporter activity.¹³

Statistical analysis

SPSS software (version 13.0, IBM Corporation, Armonk, NY, USA) was used to analyse statistics. Data from at least triplicate analysis was presented as mean \pm SEM. Student's *t* test was employed to assess the statistical significance of the differences between experimental groups; *P*-values less than 0.05 was termed as statistically significance.

Results

By using high-throughput RNA sequencing analysis, MetaLnc9 was found differentially expressed in OSF and normal mucosal samples (Fig. 1A). To validate this finding, qRT-PCR was used to show the upregulation of MetaLnc9 in OSF specimens (*n* = 25) compared to normal mucosal tissues (Fig. 1B). Moreover, results of Pearson correlation measures revealed that MetaLnc9 was positively correlated with various fibrosis-associated molecules, including alpha-smooth muscle actin (α -SMA), alpha-1 type I collagen (COL1A1) and fibronectin 1 (FN1) (Fig. 1C).

As shown in Fig. 2A, the expression of MetaLnc9 was elevated in fBMFs derived from OSF tissues compared to normal BMFs. During the healing processes, the α -SMA-expressing myfibroblasts migrate to the injured area and exert contraction forces to close the wound.¹⁶ As such, we examined the following features to assess the impact of

MetaLnc9 on myfibroblast activation. We showed that transwell migration ability (Fig. 2B), the expression of myfibroblast marker α -SMA (Fig. 2C), and collagen gel contraction (Fig. 2D) were all reduced when the expression of MetaLnc9 was inhibited. Additionally, accumulation of ROS has been shown to implicate in myfibroblast transdifferentiation in fBMFs and suppression of MetaLnc9 markedly declined the production of ROS (Fig. 2E).

The localization of lncRNAs has been known to be associated with their function.⁴ Here, we found that MetaLnc9 was predominantly in the cytoplasm of fBMFs (Fig. 3A). One of the previous studies has shown that MetaLnc9 regulated the TGF- β 1-induced myfibroblast transdifferentiation of corneal fibroblasts by sponging miR-143-3p,¹² which also mediates subconjunctival fibrosis.¹⁷ Hence, we examined whether MetaLnc9 physically interacted with miR-143. As shown in Fig. 3B, the complementarity between MetaLnc9 and miR-143 was identified and illustrated. Moreover, we found that the expression of miR-143 in OSF was lower compared to normal tissues using RNA sequencing analysis (Fig. 3C). In addition, results from luciferase reporter assay validated the direct relationship between MetaLnc9 and miR-143 as the activity was markedly reduced in cells co-transfected with miR-143 and wild-type MetaLnc9, while there was no difference between the mutant group and vector group (Fig. 3D).

Subsequently, we examined the effect of miR-143 on myfibroblast activities. As expected, the collagen gel contractility of miR-143-overexpressing fBMFs (Fig. 4A) was markedly suppressed (Fig. 4B). Furthermore, transwell migration (Fig. 4C) and wound healing (Fig. 4D) assays

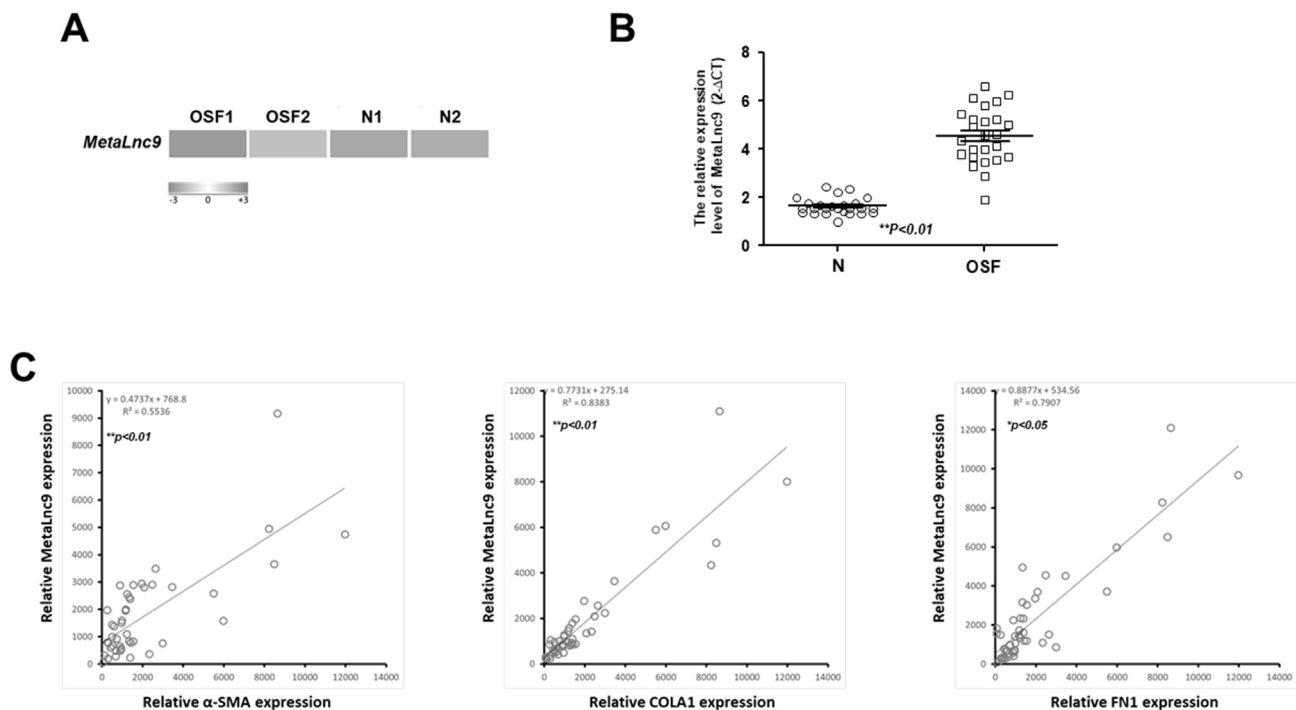


Figure 1 MetaLnc9 is overexpressed in oral submucous fibrosis tissues and positively correlated to several fibrosis-associated markers. (A) Heatmap showing differentially expressed MetaLnc9 between oral submucous fibrosis (OSF) and normal control (N) samples. (B) Quantification of MetaLnc9 in normal control and OSF tissues (*n* = 25). (C) A positive correlation was revealed between MetaLnc9 and multiple fibrosis markers, including alpha-smooth muscle actin (α -SMA), alpha-1 type I collagen (COL1A1) and fibronectin (FN1) in OSF specimens (*n* = 45) by qRT-PCR analysis.

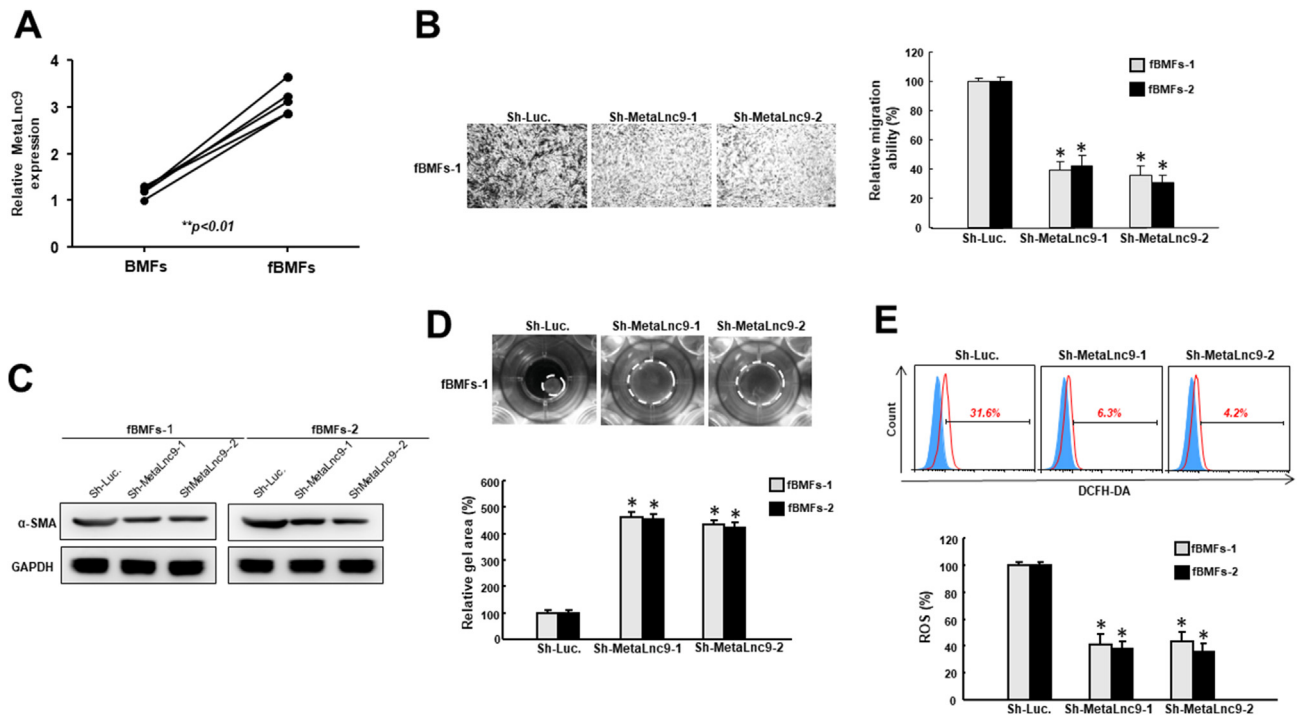


Figure 2 Inhibition of MetaLnc9 in fibrotic buccal mucosal fibroblasts attenuates multiple myofibroblast features. (A) The expression level of MetaLnc9 was upregulated in fibrotic buccal mucosal fibroblasts (fBMFs) compared to BMFs. (B) Transwell migration capacities, (C) the expression of α -SMA, (D) collagen gel contraction were all reduced in fBMFs after silencing of MetaLnc9. (E) The decreased intracellular reactive oxygen species (ROS) was detected in fBMFs with Short-hairpin (Sh)-MetaLnc9 by 2',7'-dichlorodihydrofluorescein diacetate (DCFH-DA) method.

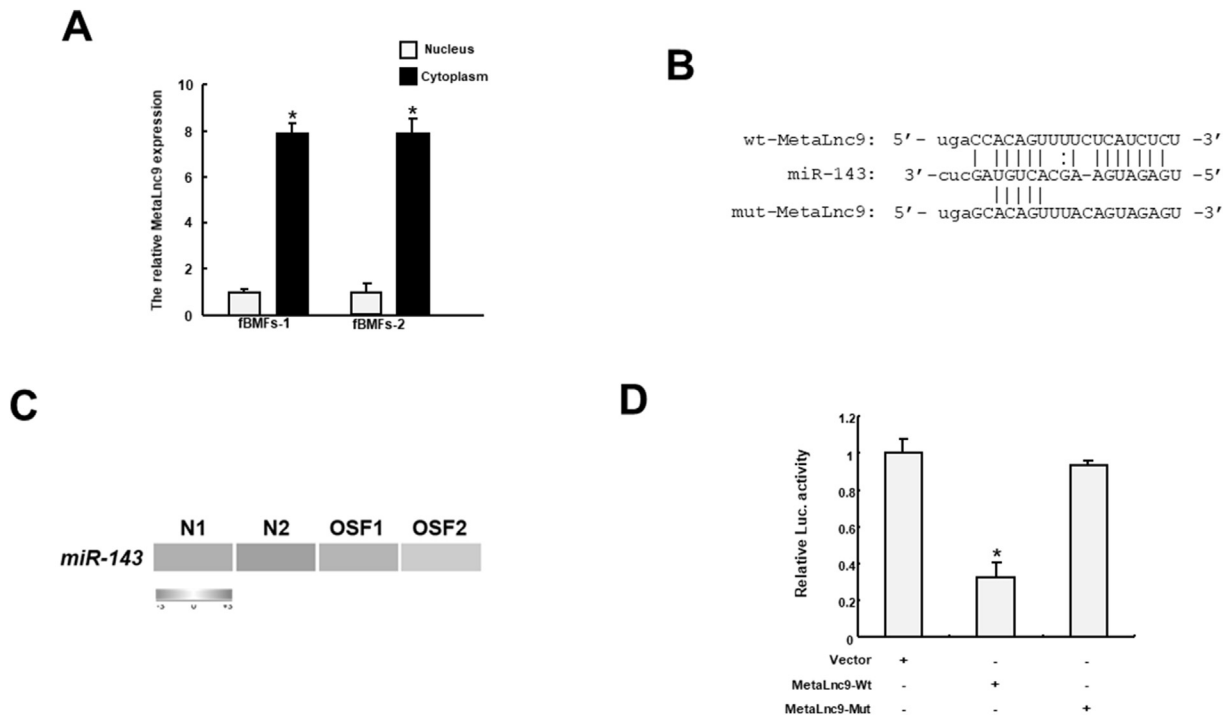


Figure 3 MetaLnc9 interacts with miR-143. (A) The relative cytoplasmic and nuclear levels of MetaLnc9 in fBMFs were analyzed by qRT-PCR. * $P < 0.05$ compared to the nucleus group. (B) Schematic representation of the alignment of the MetaLnc9 base pairing with miR-143. Wild-type (Wt) and mutated (Mut) MetaLnc9 reporter plasmids were co-transfected with miR-143 or empty vectors. (C) Repression of miR-143 was observed in OSF tissues using RNA sequencing analysis. (D) The luciferase activity of the reporter containing the wild-type MetaLnc9 was reduced by miR-143, whereas there was no effect on the activity of reporter constructs containing mutant MetaLnc9. 3' Untranslated Region (3'-UTR).

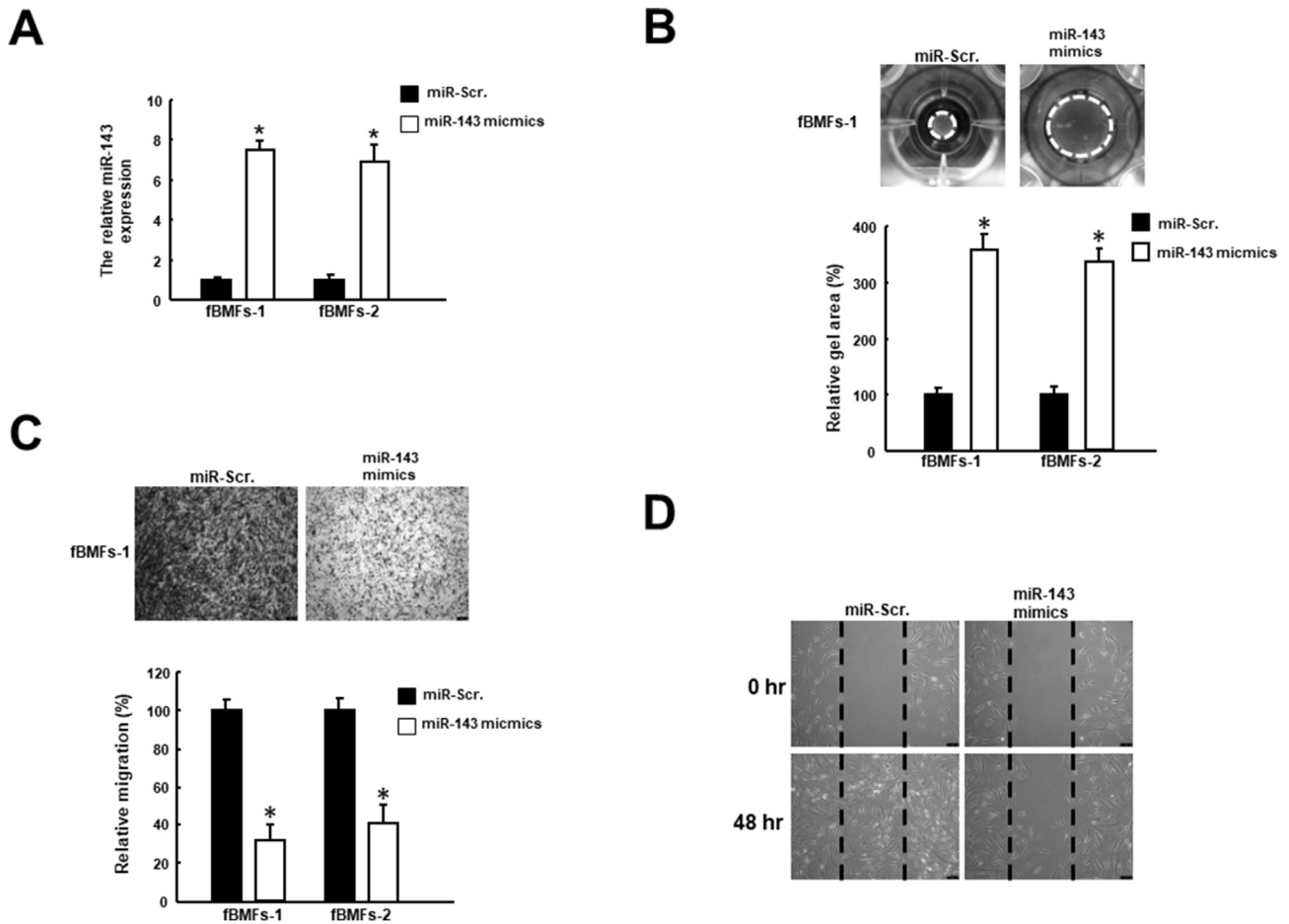


Figure 4 Overexpression of miR-143 diminishes myofibroblast phenotypes. (A) The relative expression of miR-143 in fBMFs was analyzed by qRT-PCR. Several myofibroblast activities were tested to assess the impact of miR-143, including collagen gel contraction (B), transwell migration (C), and wound healing (D) assays. * $P < 0.05$ compared to miR-Scramble (miR-Scr.).

showed that the cell motility in fBMFs was repressed when miR-143 was upregulated.

Next, we sought to verify whether the effect of MetaLnc9 on myofibroblast activities was due to direct regulation of miR-143. We showed that there was a negative relationship between MetaLnc9 and miR-143 (Fig. 5A). Besides, the reduced transwell migration ability of fBMFs following the silencing of MetaLnc9 was reversed when miR-143 inhibitor existed (Fig. 5B). Likewise, the repressive effects on collagen gel contractility (Fig. 5C) and the expression of fibrosis markers (α -SMA and COL1A1) (Fig. 5D) after silencing of MetaLnc9 was counterbalanced in the presence of miR-143 inhibitor. Taken together, these results suggested that MetaLnc9 modulates myofibroblast activities in fBMFs by directly binding to miR-143 and reducing its expression.

FSCN1 is an actin-bundling protein and is implicated in tumor cell motility and fibrosis diseases.^{18,19} A recent study has identified that FSCN1 is a key target of miR-143 for the pro-fibrotic therapy-resistant phenotype of melanoma cells.²⁰ By using bioinformatics software, we identified a potential binding site for miR-143 and illustrated the complementarity between miR-143 and FSCN1 (Fig. 6A). The subsequent luciferase reporter assay further revealed that the activity was markedly downregulated in cells

co-transfected with miR-143 and wild-type FSCN1, while there was no change in the mutant group (Fig. 6B). Besides, our results revealed that the expression of FSCN1 in fBMFs was abolished when miR-143 mimics were added (Fig. 6C). Also, we showed that the expression of FSCN1 was positively related to MetaLnc9 (Fig. 6D). Consequently, these findings indicated that MetaLnc9 may exert its pro-fibrosis property through modulation of miR-143/FSCN1 axis.

Discussion

Given the paucity of effective treatments for OSF, new insights into the mechanisms controlling BMFs activation are essential to develop new therapeutic approaches. Currently, most of the studies regarding MetaLnc9 are about its oncogenic role in various types of tumors, including oral cancer.¹¹ Accordingly, we sought to examine whether MetaLnc9 promotes the development of precancerous OSF. We found that it was upregulated in OSF tissues and positively correlated with numerous fibrosis markers. Next, we substantiated that the pro-fibrosis property of MetaLnc9 was mediated by directly binding to miR-143 and titrating its repressive effect on FSCN1. This finding was inconsistent with the work by Zhang et al. who showed that

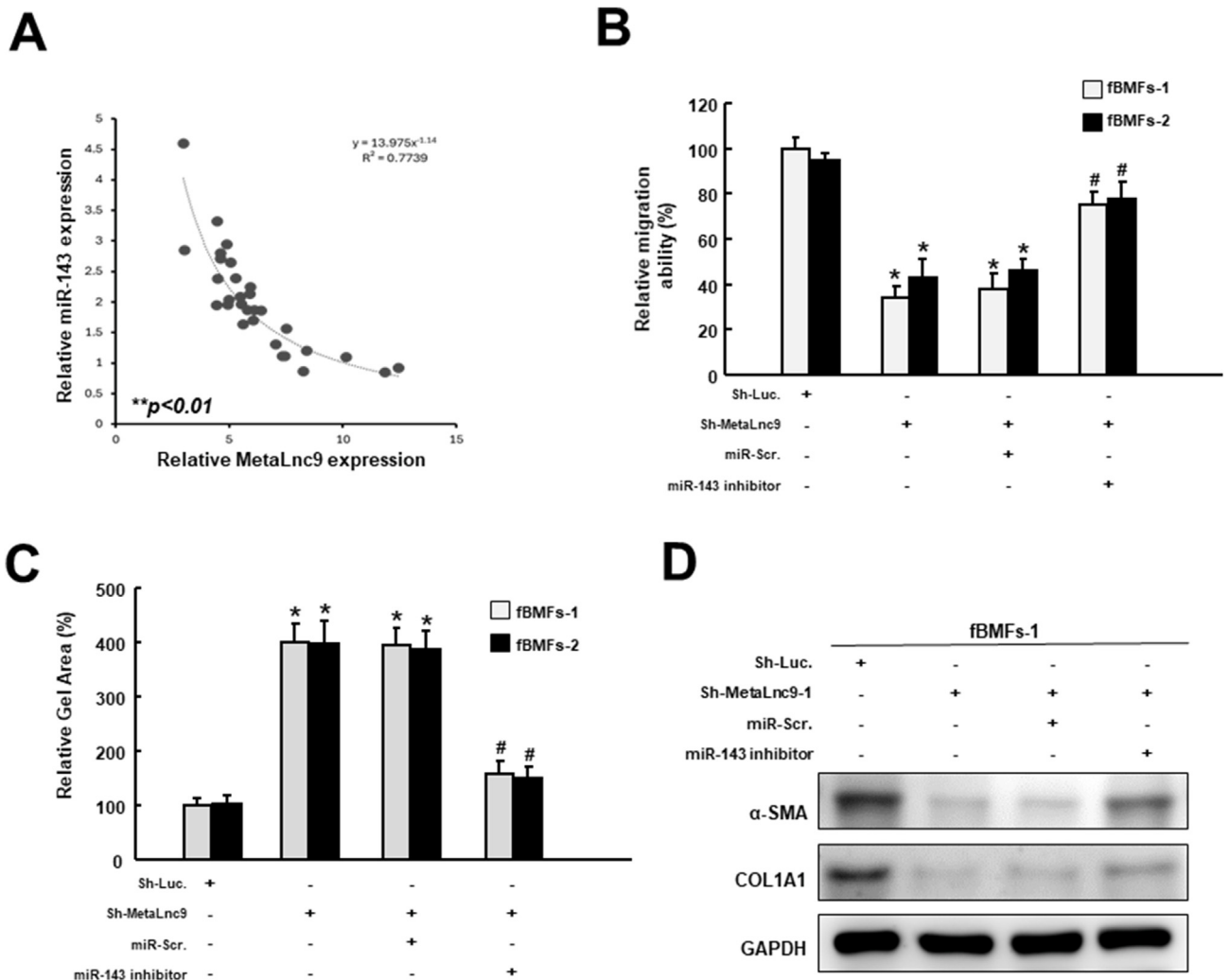


Figure 5 MetaLnc9 regulates myofibroblast characteristics through repression of miR-143. (A) The inverse relationship between MetaLnc9 and miR-143 ($n = 30$). The suppressive effects of silencing MetaLnc9 on migration capacity (B), collagen gel contractility (C), and expression of fibrosis markers (D) in fBMFs were reversed when the expression of miR-143 was reduced. * $P < 0.05$ compared to Sh-Luc. group.

MetaLnc9 exerted anti-fibrosis capacity and overexpression of MetaLnc9 diminished the TGF- β 1-elicited myofibroblast activation.¹² It appeared that MetaLnc9 can exert both anti- and pro-fibrotic properties under different conditions. Further work is required to unveil the pivotal event that determines how MetaLnc9 mediates the fates of myofibroblasts.

The significance of miR-143 and its cluster partner, miR-145, in cardiovascular and tumor biology has been addressed in multiple studies.^{21,22} Here, we showed miR-143 was downregulated in precancerous OSF tissues and possesses anti-fibrosis ability. Similar to MetaLnc9, miR-143 is involved in both pro- and anti-fibrosis processes. For instance, it has been shown that miR-143-3p overexpression enhanced the proliferation, migration, and excessive ECM accumulation of human cardiac fibroblasts by targeting sprout3, possibly contributing to myocardial fibrosis.²³ Also, miR-143 increased the expression of type III collagen in normal gastric fibroblasts and cancer-associated

fibroblasts via TGF- β /Smad signaling.²⁴ MiR-143 contributed to the TGF- β 1-induced subconjunctival and corneal fibrosis as well.^{12,17} On the other hand, overexpression of miR-143 was reported to prohibit the development of hepatic fibrosis in autoimmune hepatitis by targeting transforming growth factor β -activated kinase 1 (TAK1).²⁵ Another study showed that miR-143 suppressed the proliferation of mesangial cells and renal fibrosis by directly binding to Erb-b2 receptor tyrosine kinase 3 (ERBB3).²⁶ Besides, miR-143 has been shown to inhibit hyperplastic scar formation by targeting connective tissue growth factor (CTGF).²⁷ Along these same lines, our results demonstrated that miR-143 exhibited an anti-fibrosis effect on myofibroblast activities of fBMFs, possibly through directly binding to FSCN1.

FSCN1 is a crucial cytoskeletal regulator and an actin-bundling protein that belongs to the actin cytoskeletal protein family.²⁸ A wide range of actin-based structures to which FSCN1 contributes have been identified and are known to be required functionally for cell migration and/or

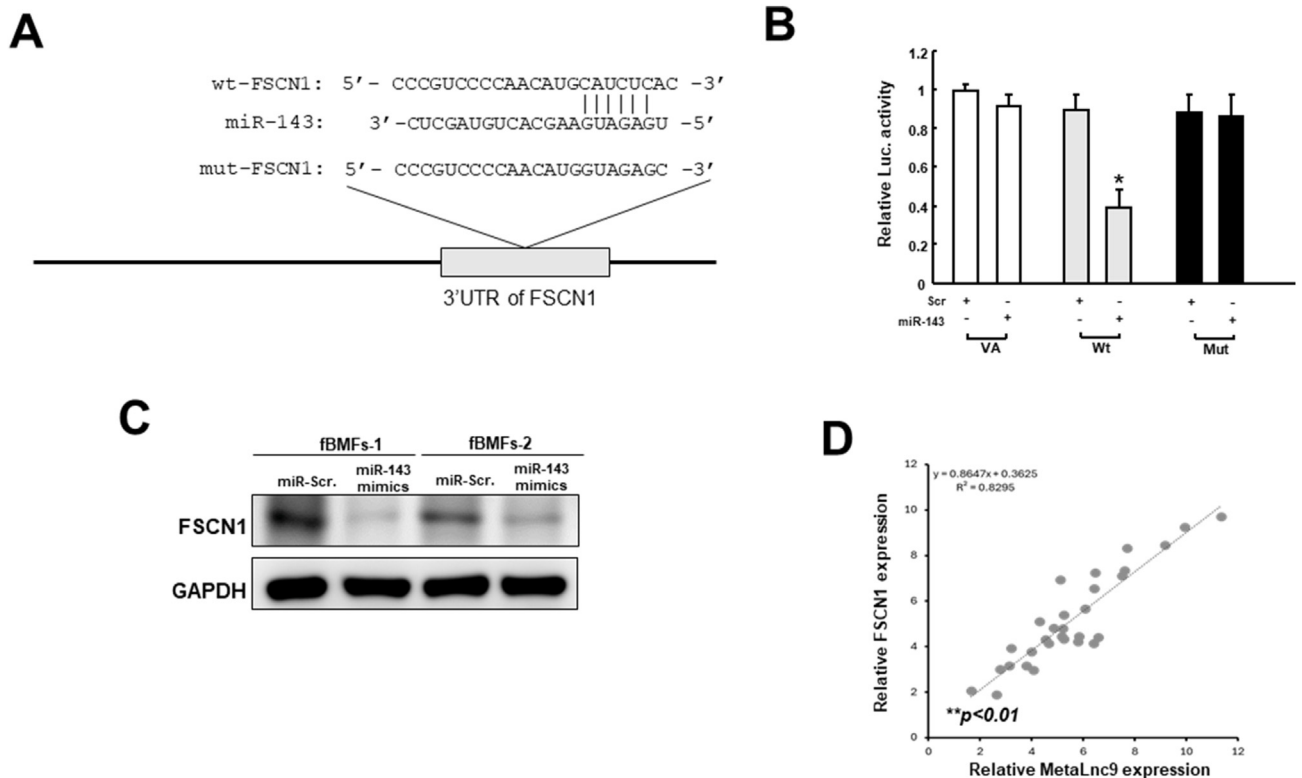


Figure 6 FSCN1 is a putative target of miR-143 and is positively associated with MetaLnc9. (A) An illustration of the 3'-UTR of full-length (wild-type, Wt) and mutated FSCN1 complementarity between the seed sequence of miR-143 predicted by the TargetScan in silico browser. (B) The luciferase activity of the reporter construct containing the wild-type FSCN1 was repressed by miR-143, whereas there was no effect on the activity of reporter constructs containing mutant (Mut) FSCN1 in BMFs. (C) The expression of FSCN1 was abrogated in fBMFs treated with miR-143 mimics. (D) A positive correlation between MetaLnc9 and FSCN1 was observed ($n = 30$). Vector alone plasmid (VA).

invasion.²⁹ Indeed, increased FSCN1 was found to stimulate the invasion, and glycolysis of oral cancer cells via the IRF4/AKT signaling.^{30,31} Moreover, it has been shown that the elevation of FSCN1 mediated epithelial-to-mesenchymal transition (EMT) since it was a downstream effector of SNAI2 in the TGF- β -induced EMT in human lung and oral cancer cells.^{32,33} Since cells undergo EMT is a major source of fBMFs,^{1,6,34,35} it is reasonable to presume that FSCN1 may contribute to the transdifferentiation of fBMFs. In line with this assumption, we did observe a positive correlation between FSCN1 and MetaLnc9. Further exploration of the direct impact of FSCN1 on myofibroblast activities is warranted in future research.

Betel nut chewing is a primary risk factor for the OSF progression.^{1,14} Notably, we found that MetaLnc9 were regulated by several areca nuts-associated transcriptional factors, including FOXC2, SP1, and STAT3 (data were not shown). Exposure to areca nut extract (ANE) significantly increased the expression of FOXC2 in oral cancer cells, which was associated with the induction of cancer stemness.³⁶ Although the directed evidence linking FOXC2 with OSF is still lacking, previous study reported that the induction of FOXC2 nuclear translocation was required for matrix stiffness-driven myofibroblastic activation of hepatic stellate cells (HSC),³⁷ implicating that ANE might promote OSF development by enhancing transcriptional

activity of FOXC2. Arecoline, the major active compound in areca nuts, induced not only mucosal fibrosis but also cardiac fibrosis by activating the TGF β /Smad/SP1 pathway.^{1,14,38} Additionally, arecoline has been demonstrated to enhance the myofibroblastic activation of BMFs and the malignancy of oral cancer cells by driving the SNAI/IL-6 and IL-6/STAT3 pathways, respectively.^{35,39} These findings indicate the importance of activating the SNAI/IL-6/STAT3 pathway in contributing to profibrogenesis of OSF and its further precancerous condition.⁴⁰ Taken together, the up-regulated MetaLnc9 could be a response for the activation of FOXC2, SP1, and STAT3 induced by areca nuts exposure. This suggests that the MetaLnc9/miR-143/FSCN1 axis might constitute a significant part of the pathological mechanism by which the areca nuts consumption facilitates OSF development. Consequently, this necessitates further investigation into the relationship between betel nut chewing habits and the expression levels of MetaLnc9 in the oral mucosal tissues of OSF patients in future studies.

In summary, we found that MetaLnc9 was elevated in OSF tissues and its pro-fibrosis property in fBMFs may be mediated by sequestering miR-143 and reducing the availability of miR-143 to FSCN1. As such, targeting MetaLnc9/miR-143/FSCN1 axis may be a therapeutic direction for the treatment of OSF through inhibiting fBMF activation.

Declaration of competing interest

All authors have no conflicts of interest relevant to this article.

Acknowledgments

The administrative and financial supports of this study were from the Chung Shan Medical University Hospital (grant number: CSH-2023-C-055), Chung Shan Medical University and Chi-Mei Medical Center, (grant number: CMCSMU11204), China Medical University (grant number: CMU112-S-47) and the Ministry of Science and Technology (grant number: MOST 108-2314-B-040 -004; MOST 109-2314-B-040-023; MOST 110-2314-B-040-030) in Taiwan.

References

- Chang YC, Tsai CH, Lai YL, et al. Arecoline-induced myofibroblast transdifferentiation from human buccal mucosal fibroblasts is mediated by ZEB1. *J Cell Mol Med* 2014;18:698–708.
- Pachera E, Assassi S, Salazar GA, et al. Long noncoding RNA H19X is a key mediator of TGF- β -driven fibrosis. *J Clin Invest* 2020;130:4888–905.
- Savary G, Dewaeles E, Diazzi S, et al. The long noncoding RNA DNM3OS is a reservoir of FibromiRs with major functions in lung fibroblast response to TGF- β and pulmonary fibrosis. *Am J Respir Crit Care Med* 2019;200:184–98.
- Statello L, Guo CJ, Chen LL, Huarte M. Gene regulation by long non-coding RNAs and its biological functions. *Nat Rev Mol Cell Biol* 2021;22:96–118.
- Yu CH, Hsieh PL, Chao SC, Chen SH, Liao YW, Yu CC. XIST/let-7i/HMGA1 axis maintains myofibroblasts activities in oral submucous fibrosis. *Int J Biol Macromol* 2023;232:123400.
- Lee YH, Liao YW, Lu MY, Hsieh PL, Yu CC. LINC00084/-miR-204/ZEB1 axis mediates myofibroblastic differentiation activity in fibrotic buccal mucosa fibroblasts: therapeutic target for oral submucous fibrosis. *J Personalized Med* 2021;11:707.
- Wang L, Han S, Jin G, et al. LINC00963: a novel, long non-coding RNA involved in the transition of prostate cancer from androgen-dependence to androgen-independence. *Int J Oncol* 2014;44:2041–9.
- Yu T, Zhao Y, Hu Z, et al. MetaLnc9 facilitates lung cancer metastasis via a PGK1-activated AKT/mTOR Pathway. *Cancer Res* 2017;77:5782–94.
- Jiao H, Jiang S, Wang H, Li Y, Zhang W. Upregulation of LINC00963 facilitates melanoma progression through miR-608/NACC1 pathway and predicts poor prognosis. *Biochem Biophys Res Commun* 2018;504:34–9.
- Wu Z, Wang W, Wang Y, et al. Long noncoding RNA LINC00963 promotes breast cancer progression by functioning as a molecular sponge for microRNA-625 and thereby upregulating HMGA1. *Cell Cycle* 2020;19:610–24.
- Lee SP, Hsieh PL, Fang CY, et al. LINC00963 promotes cancer stemness, metastasis, and drug resistance in head and neck carcinomas via ABCB5 regulation. *Cancers (Basel)* 2020;12:1073.
- Zhang L, Gao J, Gong A, et al. The long noncoding RNA LINC00963 inhibits corneal fibrosis scar formation by targeting miR-143-3p. *DNA Cell Biol* 2022;41:400–9.
- Ng MY, Yu CC, Chen SH, Liao YW, Lin T. Er:YAG laser alleviates inflammation in diabetes-associated periodontitis via activation CTBP1-AS2/miR-155/SIRT1 axis. *Int J Mol Sci* 2024;25:2116.
- Yang H-W, Chun-Yu Ho D, Liao H-Y, et al. Resveratrol inhibits arecoline-induced fibrotic properties of buccal mucosal fibroblasts via miR-200a activation. *J Dent Sci* 2024;19:1028–35.
- Chou MY, Fang CY, Hsieh PL, Liao YW, Yu CC, Lee SS. Depletion of miR-155 hinders the myofibroblast activities and reactive oxygen species generation in oral submucous fibrosis. *J Formos Med Assoc* 2022;121:467–72.
- Hinz B, Mastrangelo D, Iselin CE, Chaponnier C, Gabbiani G. Mechanical tension controls granulation tissue contractile activity and myofibroblast differentiation. *Am J Pathol* 2001;159:1009–20.
- Hwang YH, Jung SA, Lyu J, Kim YY, Lee JH. Transforming growth factor- β 1-induced human subconjunctival fibrosis is mediated by microRNA 143/145 expression. *Invest Ophthalmol Vis Sci* 2019;60:2064–71.
- Li Z, Shi J, Zhang N, et al. FSCN1 acts as a promising therapeutic target in the blockade of tumor cell motility: a review of its function, mechanism, and clinical significance. *J Cancer* 2022;13:2528–39.
- Fu H, Gu YH, Yang YN, Liao S, Wang GH. MiR-200b/c family inhibits renal fibrosis through modulating epithelial-to-mesenchymal transition via targeting fascin-1/CD44 axis. *Life Sci* 2020;252:117589.
- Diazzi S, Baeri A, Fassj J, et al. Blockade of the pro-fibrotic reaction mediated by the miR-143/-145 cluster enhances the responses to targeted therapy in melanoma. *EMBO Mol Med* 2022;14:e15295.
- Elia L, Quintavalle M, Zhang J, et al. The knockout of miR-143 and -145 alters smooth muscle cell maintenance and vascular homeostasis in mice: correlates with human disease. *Cell Death Differ* 2009;16:1590–8.
- Chen X, Guo X, Zhang H, et al. Role of miR-143 targeting KRAS in colorectal tumorigenesis. *Oncogene* 2009;28:1385–92.
- Li C, Li J, Xue K, et al. MicroRNA-143-3p promotes human cardiac fibrosis via targeting sprout3 after myocardial infarction. *J Mol Cell Cardiol* 2019;129:281–92.
- Naito Y, Sakamoto N, Oue N, et al. MicroRNA-143 regulates collagen type III expression in stromal fibroblasts of scirrhous type gastric cancer. *Cancer Sci* 2014;105:228–35.
- Tu H, Chen D, Cai C, et al. MicroRNA-143-3p attenuated development of hepatic fibrosis in autoimmune hepatitis through regulation of TAK1 phosphorylation. *J Cell Mol Med* 2020;24:1256–67.
- Bai S, Xiong X, Tang B, et al. Exosomal circ_DLGP4 promotes diabetic kidney disease progression by sponging miR-143 and targeting ERBB3/NF- κ B/MMP-2 axis. *Cell Death Dis* 2020;11:1008.
- Mu S, Kang B, Zeng W, Sun Y, Yang F. MicroRNA-143-3p inhibits hyperplastic scar formation by targeting connective tissue growth factor CTGF/CCN2 via the Akt/mTOR pathway. *Mol Cell Biochem* 2016;416:99–108.
- Ponting CP, Russell RB. Identification of distant homologues of fibroblast growth factors suggests a common ancestor for all beta-trefoil proteins. *J Mol Biol* 2000;302:1041–7.
- Hashimoto Y, Kim DJ, Adams JC. The roles of fascins in health and disease. *J Pathol* 2011;224:289–300.
- Zhang X, Feng H, Li Z, et al. Application of weighted gene co-expression network analysis to identify key modules and hub genes in oral squamous cell carcinoma tumorigenesis. *Oncotargets Ther* 2018;11:6001–21.
- Li L, Chen L, Li Z, et al. FSCN1 promotes proliferation, invasion and glycolysis via the IRF4/AKT signaling pathway in oral squamous cell carcinoma. *BMC Oral Health* 2023;23:519.
- Keshamouni VG, Jagtap P, Michailidis G, et al. Temporal quantitative proteomics by iTRAQ 2D-LC-MS/MS and corresponding mRNA expression analysis identify post-transcriptional modulation of actin-cytoskeleton regulators during TGF-beta-Induced epithelial-mesenchymal transition. *J Proteome Res* 2009;8:35–47.

33. Wang L, Jia Y, Jiang Z, Gao W, Wang B. FSCN1 is upregulated by SNAI2 and promotes epithelial to mesenchymal transition in head and neck squamous cell carcinoma. *Cell Biol Int* 2017;41:833–41.
34. Fang CY, Hsia SM, Hsieh PL, et al. Slug mediates myofibroblastic differentiation to promote fibrogenesis in buccal mucosa. *J Cell Physiol* 2019;234:6721–30.
35. Peng CY, Liao YW, Lu MY, Yang CM, Hsieh PL, Yu CC. Positive feedback loop of SNAIL-IL-6 mediates myofibroblastic differentiation activity in precancerous oral submucous fibrosis. *Cancers (Basel)* 2020;12:1611.
36. Li YC, Chang JT, Chiu C, et al. Areca nut contributes to oral malignancy through facilitating the conversion of cancer stem cells. *Mol Carcinog* 2016;55:1012–23.
37. Sun L, Li Y, Wang H, et al. FOXC2-AS1/FOXC2 axis mediates matrix stiffness-induced trans-differentiation of hepatic stellate cells into fibrosis-promoting myofibroblasts. *Int J Biol Sci* 2023;19:4206–22.
38. Ku CW, Day CH, Ou HC, et al. The molecular mechanisms underlying arecoline-induced cardiac fibrosis in rats. *Open Life Sci* 2021;16:1182–92.
39. Chuerduangphui J, Ekalaksananan T, Chaiyarit P, et al. Effects of arecoline on proliferation of oral squamous cell carcinoma cells by dysregulating c-Myc and miR-22, directly targeting oncostatin M. *PLoS One* 2018;13:e0192009.
40. Angadi PV, Rao SS. Areca nut in pathogenesis of oral submucous fibrosis: revisited. *Oral Maxillofac Surg* 2011;15:1–9.